Performance Study of an Airlift Pump with Bent Riser Tube

A.-F. MAHROUS
Mechanical Power Engineering Department
Faculty of Engineering
Menoufiya University
Gamal Abdel-Nasser St., Shebin El-Kom, 32511
EGYPT
afmahrous@hotmail.co.uk

Abstract: - Airlift pump is a type of deep well pumps. Sometimes, it is used for removing water from mines or pumping slurry of sand and water or other solutions. This work presents a numerical investigation into necessary ways to reduce momentum loss associated with local bends of the riser tube section of the airlift pump and consequently an improvement in pump performance would be attained. The investigated local tube bend are in the form of an S-shaped like duct. A numerical model of airlift pump, with bent riser tube, based on the concept of momentum balance was developed and validated against available experimental data. Parametric predictive studies on model airlift pumps with different riser tube configurations, including position, orientation, and graduation of the S-bend straight tube section, were carried out. The numerical results showed that gradually enlarging the riser tube S-bend straight section would significantly improve the airlift pump discharge rate. This is attributed to reduced acceleration loss followed the expansion of air phase in the enlarged S-bend section of the riser tube. Increasing the degree of tube expansion of the gradually enlarged S-bend straight tube section, the predicted results illustrated an improvement in the pump discharge rate that is limited by the value of tube expansion ratio. On the other hand, the numerical results showed that setting local S-bend of the riser tube at different positions from the air injector has a negligible effect on the pump performance.

Key-Words: - Airlift pumps, two-phase flow, pumping devices, bent riser tube, S-bend

1 Introduction

Airlift pumps are means of artificially lifting liquids or liquid-solid mixtures (slurries) from deep wells or vessels. Use of airlift pump has been promoted for a number of reasons such as: lower initial cost and maintenance, easy installation, small space requirements, simplistic design and construction, ease of flow rate regulation, and ability to handle corrosive, highly toxic and radioactive fluids. In the airlift system, air (or gas) is injected through an injection system at (or near) the base of a vertical pipe (the riser tube) that is partially submerged in a liquid or slurry. Bubbles, therefore, form and expand as they rise in the riser tube. A two- (or three-) phase column containing air phase has a lower density than a column of liquid alone and therefore the mixture formed in the airlift tube rises and is expelled at the top of the pump.

Numerous publications were published related to theoretical and experimental analysis of the airlift pump performance. Parker [1] made a comprehensive experimental study to determine the effects of foot piece design on the lifting characteristics of the airlift pump used for hydraulic transport of liquids. The effects of air injection method on the airlift pump performance were experimentally investigated by Mansour and Khalil [2] and by Khalil et al. [3]. It was concluded that, initial bubble size and distribution in the riser tube could have great effects on the pump performance. Khalil and Mansour [4] carried out an experimental investigation on the airlift pump performance by studying the effect of introducing a surfactant to the pumped liquid. Results showed that an improvement in the pump capacity and pump efficiency can be obtained when using a surfactant with low concentration. They studied the influence of riser tube diameter and injector design on the efficiency characteristics of the airlift pump. Mahrous [5] numerically investigated the performance of airlift pump lifting solids under various geometrical and operational conditions. The predictive studies showed that the solid particles volumetric concentration in the suction section of the airlift

tube significantly affects the airlift pump efficiency based on solids as the main gain of the pump. It has been reported that airlift pump with bent riser tube is less efficient than that of straight vertical riser tube [6]. However, in real life situations, the use of local riser tube bend or flexible riser tubes is considerably unavoidable.

It is commonly accepted that expansion of air in the riser tube of the airlift pump from the air injection pressure to the atmospheric pressure causes the two-phase air-liquid (or air-slurry) flow to distribute in a number of patterns [7]. The basic flow patterns are bubbly, slug, churn and annular flows (Fig.1). At low air input velocity, the air phase can rise in bubbles of different and variable shape and size. This type of flow is called bubbly flow. As the input air rate increases, the smaller bubbles begin to coalesce into larger bubbles or air slugs which in essence separate the water column into the slug flow regime. The transition between these two flow regimes is termed as the bubbly-slug flow regime where small bubbles are found suspended within the liquid slugs between the larger air slugs [8]. In case of very high input air velocities, the liquid can be pushed to the wall of the tube and the air streams separate in the middle of the tube and loaded with droplets of liquid. This type of flow regime is called annular flow. In annular flow, the continuity of air along the pipe appears in the core and no liquid is being lifted. Moreover, the pressure losses and power losses of flow are extremely high. So, for airlift pumps, it is advisable to avoid the ranges of annular flow, which is characterized by poor pumping efficiency. If the difference between the air injection pressure and pressure at pump outlet, which usually is atmospheric, is high, annular flow can occur in the upper part of the riser tube. While in the lower part, just above the air injection zone, bubbly flow is dominating. In such cases, the pump performance may be highly improved if the pipe diameter is enlarged at certain distances [9, 10]. This graduation of the riser tube could ensure slug flow along its height.

The main objective of this work was to numerically study the effects of riser tube configuration on the airlift pump performance. The investigated riser tube section has an S-shaped like bend. In order to reduce the pumping energy loss due to the presence of local bends on the riser tube, a gradual enlargement S-bend section was computationally made in the riser tube section. The graduated S-bend section on the riser tube was tested at different degrees of exit to inlet diameter ratio to Figure out the appropriate expansion ratio with regards to pump performance. Furthermore, the S-shaped bend section was numerically tested at different degrees of bend angles.

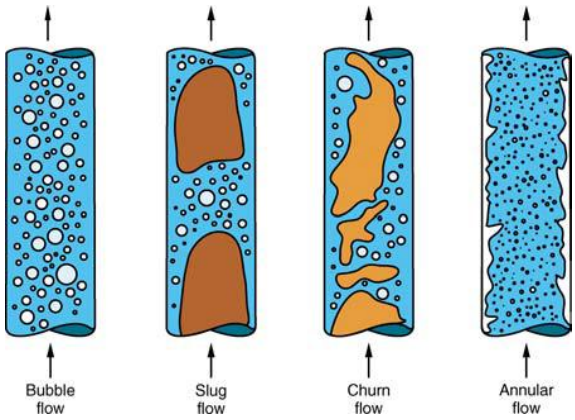

Fig.1: Flow regimes for gas-liquid two-phase flow in a vertical pipe [11].

2 Numerical Approach

Numerous studies up-to-date have offered different calculation methods of airlift pump performance based on the principles of theoretical treatment. Among others, Clauss [12], Boës *et al*. [13], Yoshinaga and Sato [14], Margris and Papanikas [15], and Hatta *et al*. [16] developed more reliable theoretical analysis for the calculations of airlift pumps. Each of these models allowed a general calculation for the pumping action required by the airlift pump. In the present work, a numerical analysis of the performance of airlift pump based on the principle of momentum balance is presented under steady state operating conditions. The airlift pump performance is studied according to the analysis of Yoshinaga and Sato [14]. The assumptions made for the mathematical formulation of the airlift mechanism were: compressible and ideal gas flow for the air phase, the planes of equal velocity and equal pressure are normal to the pipe axis (this makes the problem one-dimensional), no exchange of mass between phases, and isothermal flow for all phases. The assumption of isothermal flow is justified only if the phases flow slowly through the airlift tube so that a continuous heat exchange with the environment is no longer possible, Margaris and Papanikas [15].

A schematic diagram of the proposed model of the air lifting system is shown in Fig.2. The body of

the airlift pump illustrated in Fig.2 consists of two main parts. The first lower part is a suction pipe of length (L_S) between the bottom end (level E) and the air injection ports (level I), while the second part is the riser tube of length (L_R) between the compressed air and discharge ports. A model S-shaped bend tube section of straight tube length (L_B), bend angle (θ), and of an expansion ratio ($\beta = D_D/D_U$) was set at some points on the riser tube in order to investigate its effect on the pump discharge rate. The ratio between the riser tube section length upstream of the S-bend section (L_U) and the total riser tube length (L_R) is termed as (γ). Compressed air is injected at a water depth of (L_I). The ratio between the submerged depth (L_I) and the total riser tube length (L_R) is termed as the submergence ratio (α).

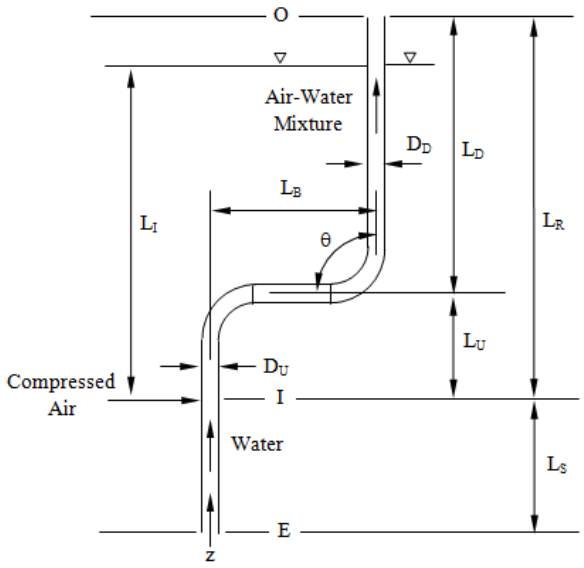

Fig.2: Model of numerically tested airlift pump.

Applying the concept of momentum balance to a control volume bounded by the pipe wall and pipe cross sections at the suction and discharge levels (levels E and O, respectively) results in the momentum equation.

$$
\begin{aligned}
&A_U \rho_L j_L u_{L,E} - A_D\left(\rho_{G,O} j_{G,O} u_{G,O} + \rho_L j_L u_{L,O}\right) \\
&- \pi D_U \int_E^I \tau_L \, dz \\
&- \left[\pi D_U \int_I^U \tau_2 \, dz + \pi \int_U^D D_z \, \tau_2 \, dz \right. \\
&\left. + \pi D_D \int_D^O \tau_2 \, dz\right] \\
&- A_U \int_E^I \rho_L \varepsilon_L g \, dz \\
&- \left[A_U \int_I^U \left(\rho_G \varepsilon_G + \rho_L \varepsilon_{L,2}\right) g \, dz \right. \\
&- \int_U^D \left(\rho_G \varepsilon_G + \rho_L \varepsilon_{L,2}\right) A_z g_z \, dz \\
&\left. + A_D \int_D^O \left(\rho_G \varepsilon_G + \rho_L \varepsilon_{L,2}\right) g \, dz\right] \\
&+ \int_U^D (P_z \, dA_s)_z \\
&+ [A_U\{P_O + \rho_L g(L_S + L_I)\} - A_D P_O] = 0
\end{aligned}
\tag{1}
$$

Here ρ is the density, j is the volumetric flux, u is the velocity, A is pipe cross-sectional area, D is pipe diameter, τ is the shear stress, ε is the volumetric fraction, P is the pressure, and g is the acceleration due to gravity. The subscripts L and G denote the liquid and gas phases, respectively. In addition, the subscripts s, z and 2 respectively refer to the surface area, co-ordinate z, and the two-phase air-water mixture. The upstream and downstream of the S-shaped bend test section are referred to by the subscripts U and D, respectively.

In Equation 1, the first and second terms denote the momentum of flow that enters through E and leaves through O, the third and fourth terms denote the frictional forces in the suction and riser tubes, respectively, the fifth and sixth terms denote the weight of the water phase (in the suction tube) and the weight of the two-phase air-water mixture (in the riser tube), the seventh term denotes the flow

direction component of pressure force acting on the surface of the S-shaped bend section, and the eighth term includes the hydrostatic pressure force of the surrounding water, acting at the bottom end of the pipe at section E. It is noted that the interaction forces between phases, such as the drag and virtual mass forces, appear in the mathematical formulation only if the conservation equations of mass and momentum are applied for each phase separately. Here, the mean velocity of the component "*i*" (*i* is air or water) is given as:

$$u_i = \frac{j_i}{\varepsilon_i} \tag{2}$$

Since both the air pressure and airflow rate vary throughout the pump, owing to the expansion of air, the frictional and body forces in the riser tube section cannot be estimated at the mid section of the riser tube and, therefore, the riser tube should be divided into a number of short segments in the flow direction. The length of each segment is chosen such that the nodes pressure ratio for any segment is the same for all segments. Assuming that the pressure distribution for each segment is linear, the frictional pressure gradient at such a segment and the flow local conditions are calculated at the middle of this segment. The terms of frictional and body forces in the momentum equation, Equation 1, are then calculated using step-by-step integration procedure throughout the riser tube.

An iterative solution is required for the calculation of air and water volumetric ratio and also for the other flow parameters that are involved in the momentum equation. The absolute hydrostatic pressure at the injection point is calculated as a necessary step to obtain both the eighth term included in the momentum equation, Equation 1, and the number of segments by which the riser tube section is divided. At that time, the length of each segment of the riser tube is to be calculated from the gradient of the hydrostatic pressure curve and the assigned value of nodes pressure ratio. Then, the absolute hydrostatic pressure at each node is calculated. The first iterative loop is the loop that assigns the airflow rate at the injection section (pump input). For each rate of airflow assigned at the injection zone, the pressure at each node of the riser tube is assumed, as a first iteration, to be equal to the hydrostatic pressure at this node. Depending on the selected value of the assigned airflow rate, the air density and air volumetric flux distributions throughout the riser tube section are calculated. The volumetric flux of the discharged water (pump output) is then introduced through a one more iterative loop. The calculations are, then, taken place in the single-phase flow section (suction tube) to obtain the volumetric fraction of the water-phase and subsequently the body force and pressure loss term in that section. This yields later to the calculations of the first, third, and fifth terms that are included in the momentum equation. In addition, the volumetric fractions of the air and water phases are computed at sections "I", "U", "D", "O", as well as at the mid section of each segment of the riser tube. Thereafter, the various gravitational forces and pressure loss terms in the two-phase air-water flow field are computed to aid in the calculations of the second, fourth, sixth, and seventh terms in the momentum equation. The next step is the checking for the satisfaction of the momentum equation. If the momentum equation is satisfied, then a modified value of the pressure at the air injection section is calculated and subsequently modified distributions of pressure, air density, and air volumetric flux at each node of the riser tube section are obtained. The path of the calculations is therefore turned to the beginning of the water volumetric flux looping and repeated till an accurate value of the air injection pressure is reached. At this instance, as all system variables (including pump output) are explicitly computed, secondary results may be easily determined, displayed and stored in data files. After that, another value of airflow rate is assigned from its loop and the procedure of solution is repeated again. If there is no proper value of water output rate that could satisfy the momentum equation, then the assigned value of airflow rate does not represent an operational point in the performance charts.

During the calculations, the air temperature at the injection point is assumed to be the same as the temperature of the water. Moreover, the temperature gradient is neglected through the riser tube. Therefore, an isothermal expansion of gas from the air injection pressure to the pump outlet pressure (P_O) is applied. Performing the momentum balance over the entire length of the airlift tube, the airflow rate ($j_{G,O}$) aimed to achieve a specific gain of water output rate (j_L) can be numerically predicted. The numerical computations are also necessary for calculating the variations in air and water conditions throughout the individual sections of the airlift tube. Detailed information about the definition of different terms of Equation 1 can be found in the analysis of Yoshinaga and Sato [14] and in the research work of Mahrous [17].

3 Numerical Results and Discussion

3.1 Numerical Model Validation

In an attempt to verify the validity of the present modelling approach, the predicted results obtained by the developed numerical model were compared with the experimental data measured by Weber and Dedegil [18] and Yoshinaga *et al.* [14, 19] for vertically straight riser tubes, and with measurements of Fujimoto *et al.* [6] in case of riser tube with local bends. The theoretical predictions and the experimental data of the performance of airlift pump while lifting pure water have been compared through Fig.3, Fig.4, and Fig.5 at uniform tube cross-sectional area and at different values of submergence ratio (α). Figures 3, 4 and 5 show a typical example of the water pumped rate (water volumetric flux, $j_L = Q_L / A_U$, where A_U is the uniform cross sectional area of riser tube diameter D_U) as a function of air supplying rate calculated at standard atmospheric conditions (air volumetric flux, $j_{Ga} = j_{G,O} = Q_{G,O} / A_U$). For each degree of submergence ratio, the airflow was systematically varied and the corresponding water flow rates were numerically predicted. As illustrated in Fig.3, for a constant value of submergence ratio, the water flow rate increases by increasing the airflow rate. Depending on the degree of pump submergence, such behaviour continues until a limiting point is reached, where the water flow rate reaches a maximum value. Further increase in the airflow rate causes a decrease in the water flow rate. This reduction in the water flow rate can be attributed to the fact that the flow pattern in the riser tube at higher rates of airflow tends to become annular. At lower airflow rates, however, slug flow regime is dominating in the airlift tube. In the bubbly-slug flow regime, the water pumped rate is directly proportional to the airflow rate [20]. The results for the presented submergence ratios indicate a common pattern of variation. It is clear that, the submergence ratio has a strong effect on the lifting characteristics of the airlift pump. As illustrated in Fig.3, Fig.4, and Fig.5, the performance of airlift pump is well predicted by the developed numerical code over the entire range of presented submergence ratios and in both straight and bent riser tube configurations. The comparison between the numerical and measured data, thus, demonstrates a high degree of agreement that is sufficient to justify the use of this simulation tool for parametric predictive studies.

In the following subsection, unless otherwise mentioned, a model airlift pump having specifications of D_U = 18 mm, S-bend test length (L_B) = 61 mm, riser length (L_R) = 2.4 m, suction length (L_S) = 0.8 m, γ = 0.25, bend angle (θ) = 90°, expansion ratio (β) = 1, and Submergence Ratio (α) = 70% is numerically investigated.

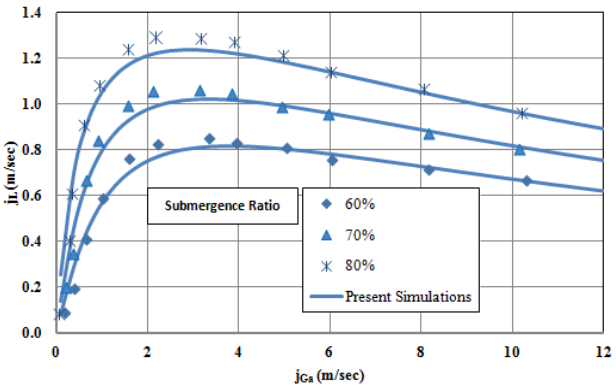

Fig.3: Comparison of numerical results calculated based on present theoretical model with experimental data by Yoshinaga *et al.* [14, 19]. Experimental conditions are: $D_U = D_D$=26 mm, L_R=6.74m, and L_S=1.12m.

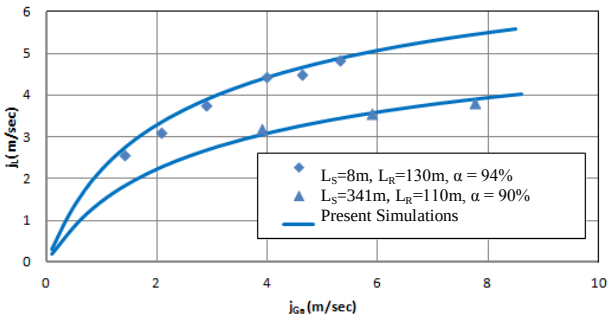

Fig.4: Comparison of numerical results calculated based on present theoretical model with experimental data by Weber and Dedegil [18]. Experimental conditions are: $D_U = D_D$=300mm.

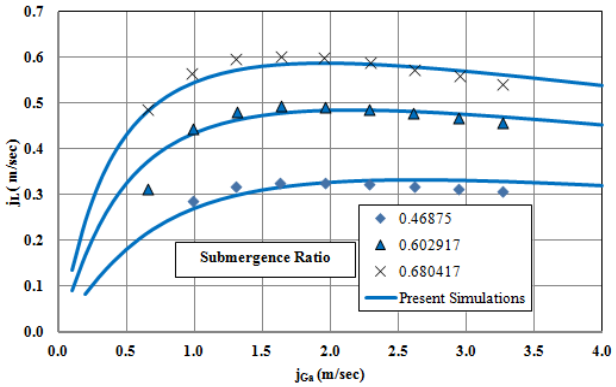

Fig.5: Comparison of numerical results calculated based on present theoretical model with experimental data by Fujimoto *et al*. [6]. Experimental conditions are: local bends on the riser section, $D_U = D_D = 18$ mm, L_R=2.4m, L_S=0.8m, L_B=0.61m, and $\gamma = 0.1833$.

3.2 Effect of Bend Section Configuration

Fig.6 (a and b) shows the water volumetric flux against the air volumetric flux at different degrees of expansion ratio (β) of the S-bend tube section. In this case, the S-bend tube section was set at 25% of the γ-ratio and the pump was run under 70% submergence ratio. In addition, the upstream diameter (D_U) and the bend tube straight section length (L_B) were kept at 18mm and 0.61m, respectively. As depicted in Fig.6a, it is clear that for reasonably low air flow rates, the water discharge rate is not appreciably influenced by the expansion ratio. For higher airflow rates, however, the pump output is improved when increasing the degree of S-bend tube expansion ratio as compared to the case of uniform diameter S-bend tube. This behaviour could be attributed to the fact that at low air flow rates, bubbly flow regime dominated in the riser tube, while at higher airflow rates, the flow pattern tends to become annular. Increasing riser tube diameter of the S-bend straight section helps minimize the acceleration loss that is accompanied by large values of air void fraction. As the degree of S-bend tube expansion ratio increases, there would be a corresponding increase in the water pumping rate but with uneven incremental increase. The incremental increase in the pump water discharge rate is decreasing as the expansion ratio increases. This suggests a limitation for the degree of the expansion ratio beyond which flow separation could take place in the riser tube.

Results in Fig.6a also illustrate that the water pumped rate in case of model airlift pump with higher degrees of bend tube expansion ratio continues to increase beyond the air flow rate at the point of maximum water pumped rate in case of model airlift pump with local bend of uniform cross section. Increasing the diameter of the S-bend straight section by 75 %, for example, increases the maximum water discharge rate by about 25% as compared to the case with uniform bend cross section (see Fig.6b).

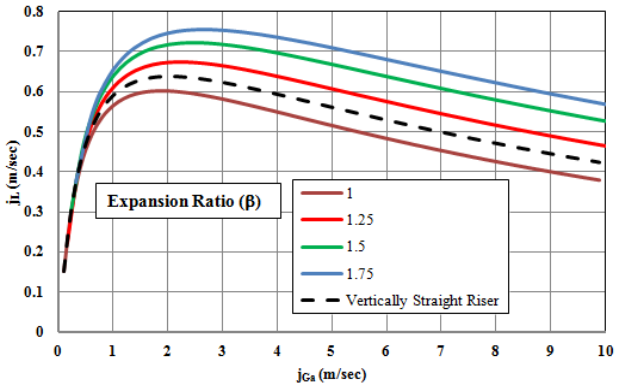

(a)

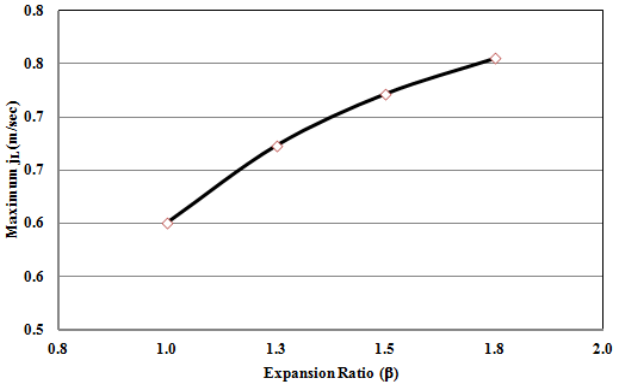

(b)

Fig.6: Effects of bend expansion ratio (β) on water discharge rate (a) and maximum pump discharge (b) (L_B=0.61m, D_U=18 mm, α=70%, and $\gamma = 0.25$).

The development of air phase in the riser tube at different degrees of S-bend β ratio is shown in Fig.7 in terms of variations in the gas holdup at j_{Ga}(based on diameter D_U)=5 m/sec. For a constant value of the expansion ratio, the gas holdup is gradually increasing as the air rises in the riser tube. Results in Fig.7 demonstrate that gradually enlarging the S-bend straight section of the riser tube decreases the volumetric fraction of the gas phase along the riser tube and therefore reduces the acceleration loss. Incremental reduction in the air volumetric fraction due to bend tube expansion is high at lower degrees of tube expansion ratio. As explained earlier, increasing the degree of S-bend tube expansion ratio could cause flow separation due to adverse pressure gradient in the diffusing section.

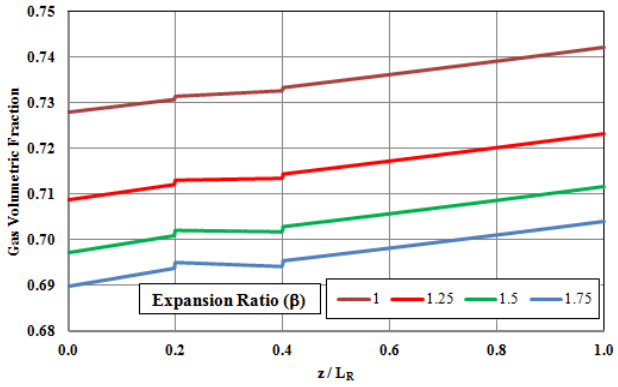

Fig.7: Variation of gas volumetric fraction along flow path line of the riser tube for the case of non-uniform S-bend cross section at j_{Ga}(based on D_U)=5 m/s (L_B=61mm, D_U=18mm, α=70%, and γ = 0.25).

Fig.8 shows the predicted effect of the S-bend section orientation on the pump discharge rate. Three S-bend sections with uniform cross-sectional area and having same projected distance of 0.61m were numerically tested at different bend angles. As can be seen in Fig.8, the water-pumping rate is improved to some extent by increasing the degree of bend angle. This can be attributed to the reduced energy loss associated with large bend angles and reduced tube total length over which frictional resistance of flow takes place.

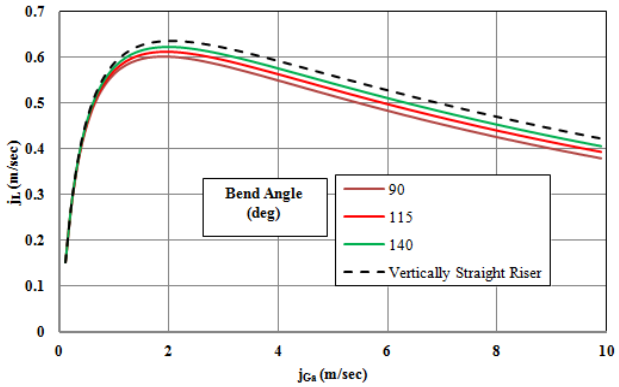

Fig.8: Effects of bend angle (θ) on water discharge rate (D_U=18mm, γ=25%, β = 1, and α=70%).

The effect of the bend section position (the γ-ratio) on the pump discharge rate at 70% of submergence ratio is predicted and plotted in Fig.9. The S-bend section with a uniform diameter was numerically located at three different positions from the injection level, namely at 25%, 50%, and 75% of the riser tube height. As depicted in Fig.9, the position of the S-bend section of the riser tube has a negligible effect on the pump performance. It is worth noting that data measured by Mahrous [21] demonstrated the same result. Although slight improvement in the water-pumping rate can be obtained when setting the S-shaped bend section close to the air injection level, the effect of bend section position of the riser tube under the current specified working conditions has an insignificant contribution to the improvement in the pump discharge rate. Fig.10 illustrates variations in the air volumetric fraction along the riser tube at different vertical positions of the bend section and at a constant value of j_{Ga}. As shown in Fig.10, the variation in air volumetric fraction due to expansion of air is not considerable. All cases almost exhibit same flow regime at pump exit section.

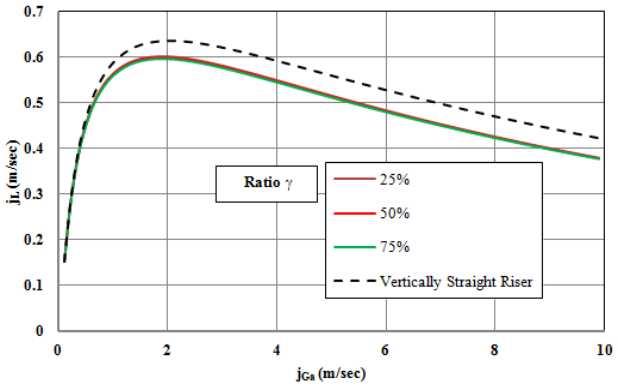

Fig.9: Effects of the γ-ratio on the water discharge rate (L_B=0.61m, D_U=D_D=18mm, and α=70%).

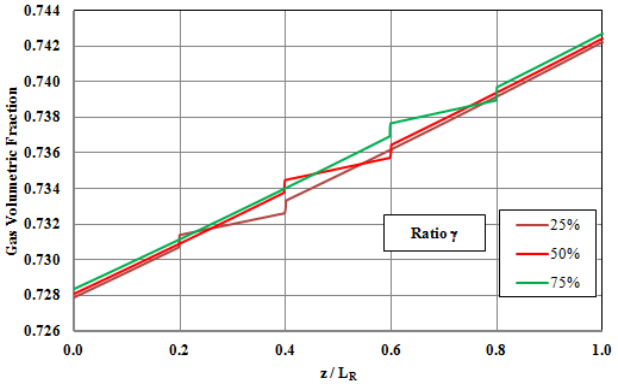

Fig.10: Variation of gas volumetric fraction along the riser tube at different S-bend positions where j_{Ga}=5 m/s (L_B=61mm, D_U=18mm, α=70%, and β = 1).

4 Conclusions

The performance of airlift pumps depends mainly on two groups of parameters. The first group is the geometrical parameters such as pipe diameter, pump height, design of injection system, and entrance geometry of the lifting pipe, while the other group is the operational parameters like the submergence ratio, injected gas flow rate and its corresponding pressure, and nature of lifted phase. This research presents a numerical predictive study of the effects of riser tube configuration on the airlift pump performance. Changing diameter, position, and tube orientation of riser pipe local S-bend straight tube section of the airlift pump was numerically investigated. The numerical model was assessed and verified through a comparison with available experimental data. Numerical results presented so far showed that the airlift pump performance is improved by gradually enlarging the straight tube section of the S-shaped bend of the riser tube. The results additionally proved an improvement in the pump discharge rate when increasing the angle of the S-bend tube section.

References

[1] Parker, G.J., *The effect of foot piece design on the performance of a small diameter airlift pump.* Int. J. Heat and Fluid Flow, 1980. **2**(4): p. 245-252.

[2] Mansour, H. and M.F. Khalil, *Effect of air injection method on the performance of airlift pump.* Mansoura Eng. J., 1990. **15**(2): p. 107-118.

[3] Khalil, M.F., Elshorbagy, K. A., Kassab, S. Z. and Fahmy, R. I., *Effect of air injection method on the performance of an airlift pump.* Int. J. Heat and Fluid Flow, 1999. **20**: p. 598-604.

[4] Khalil, M.F. and H. Mansour, *Improvement of the performance of an airlift pump by means of surfactants.* Mansoura Eng. J., 1990. **15**(2): p. 119-129.

[5] Mahrous, A.-F., *Numerical Study of Solid Particles-Based Airlift Pump Performance.* WSEAS Transactions on Applied and Theoretical Mechanics, 2012. **7**(3): p. 221-230.

[6] Fujimoto, H., Murakami, S., Omura, A., and Takuda, H., *Effect of local pipe bends on pump performance of a small air-lift system in transporting solid particles.* International Journal of Heat and Fluid Flow, 2004. **25**: p. 996–1005.

[7] Shimizu, Y., Tojo, C., Suzuki, M., Takagaki, Y. and Saito, T., *A study on the air-lift pumping system for manganese nodule mining*, in *Proc. of the 2nd International Offshore and Polar*

Engineering Conference. 1992: San Francisco, USA. p. 490-497.

[8] Reinemann, D.J. and M.B. Timmons, *Predicting oxygen transfer and total dissolved gas pressure in airlift pumping.* Aquacultural Engineering, 1989. **8**: p. 29-46.

[9] Dedegil, M.Y., *Principles of airlift techniques*, in *Encyclopedia of Fluid Mechanics*, N.P. Chereimisinoff, Editor. 1986, Gulf, Houston, TX. p. Chapter 12.

[10] Nenes, A., Assimacopoulos, D., Markatos, N. and Mitsoulis, E., *Simulation of airlift pumps for deep water wells.* The Canadian Journal of Chemical Engineering, 1996. **74**: p. 448-456.

[11] Mudde, R.F., *Gravity-driven bubbly flows.* Annu. Rev. Fluid Mech., 2005. **37**: p. 393–423.

[12] Clauss, G.F., *Investigation of characteristic data of air lifting in ocean mining (Untersuchung der kenngrőben des airlifts beim Einsatz im ozeanbergbau).* Erdől-Erdgas-Zeitschrift, 1971. **87**: p. 57-66 (In German).

[13] Boës, C., Düring, R. and Wasserroth, E., *Airlift as a drive for single and double pipe conveying plants (Airlift als antrieb für einrohr-und doppelrohr-főrderanlagen).* fördern und heben, 1972. **22**(7): p. 367-378 (In German).

[14] Yoshinaga, T. and Y. Sato, *Performance of an air-lift pump for conveying coarse particles.* Int. J. Multiphase Flow, 1996. **22**(2): p. 223-238.

[15] Margaris, D.P. and D.G. Papanikas, *A generalized gas-liquid-solid three-phase flow analysis for airlift pump design.* Trans. of the ASME, J. of Fluids Engineering, 1997. **119**: p. 995-1002.

[16] Hatta, N., Fujimoto, H., Isobe, M. and Kang, J., *Theoretical analysis of flow characteristics of multiphase mixtures in a vertical Pipe.* Int. J. Multiphase Flow, 1998. **24**(4): p. 539-561.

[17] Mahrous, A.-F., *Performance of airlift pumps*, in *Mechanical Power Engineering Dept.* 2001, Menoufiya University, Egypt.

[18] Weber, M. and Y. Dedegil, *Transport of solids according to the air-lift principle*, in *Proc. 4th International Conf. on the Hydraulic Transport of Solids in Pipes*. 1976. p. H1-1 - H1-23.

[19] Yoshinaga, T., Sato, Y. and Sadatomi, M., *Characteristics of air-lift pump for conveying solid particles.* Jap. J. Multiphase Flow, 1990. **4**: p. 174-191 (in Japanese).

[20] Lawniczak, F., Francois, P., Scrivener, O., Kastrinakis, E.G. and Nychas, S.G., *The efficiency of short airlift pumps operating at low submergence ratios.* The Canadian Journal of Chemical Engineering, 1999. **77**: p. 3-10.

[21] Mahrous, A.-F., *Experimental Study of Airlift Pump Performance with Local Bends on the Riser Tube.* In Preperation, 2012.

List of Symbols

***Roman Symbols*:**

A	Pipe cross sectional area.
D	Pipe diameter.
g	Acceleration due to gravity.
j	Average volumetric flux.
L_B	Length of S-bend tube section.

L_D Riser tube length downstream of the S-bend section.

L_I Submergence height.

L_R Riser tube length.

L_S Suction tube length.

L_U Riser tube length upstream of the S-bend section.

P Pressure.

Q Volumetric flow rate.

u Velocity.

z Elevation of the mixture level in the pipe.

***Greek Symbols*:**

α Submergence ratio (L_I / L_R).

β Expansion ratio (D_D / D_U).

ε Volumetric fraction.

γ Ratio (L_U / L_R).

θ Bend angle.

ρ Density.

τ Shear stress.

***Subscripts*:**

2 Two-phase air-water mixture.

a Atmospheric conditions.

B S-bend section.

D Downstream of bend.

E Pipe inlet section.

G Gas (air) phase.

i Index denotes the type of phase.

L Liquid (water) phase.

O Pipe outlet section.

s Surface.

U Upstream of bend.